Internal and forced ocean variability in the Mediterranean Sea

Roberta Benincasa[1], Giovanni Liguori[2,3], Nadia Pinardi[1,3], and Hans von Storch[4]

[1]University of Bologna, Department of Physics and Astronomy, Bologna, Italy
[2]University of Bologna, Department of Biological, Geological, and Environmental Sciences, Bologna, Italy
[3]Centro EuroMediterraneo sui Cambiamenti Climatici, Lecce, Italy
[4]Helmholtz-Zentrum Hereon, Institute for Coastal Systems, Geesthacht, Germany

Correspondence: Roberta Benincasa (roberta.benincasa2@unibo.it)

Abstract. Two types of variability are discernible in the ocean: a response to the atmospheric forcing and the so-called internal/intrinsic ocean variability, which is associated with internal instabilities, nonlinearities and the interactions between processes at different scales. Producing an ensemble of 20 multi-year ocean simulations of the Mediterranean Sea, initialized with realistic initial conditions, but using the same atmospheric forcing, the study examines the intrinsic variability in terms of its spatial distribution and seasonality. In general, the importance of the external forcing decreases with depth but dominates in extended shelves such as the Adriatic Sea and the Gulf of Gabes. In the case of temperature, the atmospheric forcing plays a major role in the uppermost 50 m of the water column during summer and the uppermost 100 m during winter. Additionally, intrinsic variability displays a distinct seasonal cycle in the surface layers, with a prominent maximum at around 30 m depth during the summer probably connected to the summer thermocline formation processes. Concerning current velocity, the internal variability has a significant influence at all depths.

1 Introduction

High-resolution numerical ocean models are currently employed in operational ocean forecasting, providing short-term forecasts with a lead time of 14 days for both global and regional seas, as described by Le Traon et al. (2019) and Coppini et al. (2023). Consequently, comprehending the uncertainties associated with these forecasts is crucial for enhancing future ocean forecasting. Model uncertainties restrict the duration for which accurate predictions can be made and hinder the practical applications that rely on these forecast products.

Lorenz (1975) identified two types of uncertainties affecting predictability in the climate system: the predictability of the first kind derives from the resolution of an initial value problem, i.e. predicting future states of the system given the same external forcing and different initial conditions, whereas the predictability of the second kind is connected to the boundary value problem and deals with the response of the system to changes in the external forcings. In the uncoupled ocean prediction problem, the predictability of the second kind is connected to the atmospheric fluxes at the air-sea interface while the predictability of the first kind is connected to the mesoscale and submesoscale flow field that in turn is generated by mean flow instabilities and eddy-mean flow interaction processes (Soldatenko and Yusupov (2017)).

The understanding of how internal variability can affect climate predictability, and justify the observed red profile of the cli-

25 mate variance spectra, was first achieved by Hasselmann (1976). Concurrently, mesoscale eddies and flow instabilities were mapped for the first time in the ocean (Harrison and Robinson (1978), McWilliams (1996)) and the presence of intense ocean internal variability was verified to exist. To demonstrate the importance of internal variability in climate models, Hasselmann formulated a stochastic climate model whose main assumption is that the climate system may be divided into rapidly varying, random components and a slowly responding part. Climate variability is then shown to be due to the internal random

30 components. The slow component behaves as an integrator of these inputs, whereas the fast component supplies the slow component with energy allowing the existence of internal variability in the climate system. Moreover, Hasselmann proved that climate variability would grow indefinitely without a stabilizing internal feedback mechanism. Consequently, the investigation of climate variability must be shifted from looking for positive to negative feedbacks that allow the climate system to reach stationarity in the absence of any external forcing.

35 The *internal variability*, or equivalently *intrinsic* or *stochastic* variability, is ubiquitous in the climate system and it is due to both the nonlinearity and the numerous degrees of freedom of climate itself (von Storch et al. (2001)). Understanding the internal variability enables us to statistically determine if a change is consistent with internal variability or instead at least partly related to external factors. Investigations on internal ocean variability with an ensemble approach were first found in literature starting in the 2000s when eddy-resolving global ocean models were introduced (Jochum and Murtugudde (2004),

40 Jochum and Murtugudde (2005), Arbic et al. (2014), Sérazin et al. (2015), Bessières et al. (2017), Leroux et al. (2018)). The first extensive study on the role of internal variability in the global ocean was done by Penduff et al. (2018). They showed that mesoscales compose the ocean stochastic elements of the climate system and highlighted the necessity to adopt ensemble methods. Moreover, they showed that in several areas the internal ocean variability is more significant than atmospheric variability as a contribution to climate variability for both "the low-frequency variability and the long-term trends of regional

45 ocean heat content". Similarly, in the study by Hogan and Sriver (2019) it was shown that internal variability is fundamental in setting the time scale for the ocean temperature adjustment process, increasing the speed at which the ocean takes up heat from the atmosphere, that is instead highly underestimated by just considering atmospheric variability. Lastly, as regards the scale dependency of the internal variability, it was demonstrated by Tang et al. (2019) that by increasing the horizontal spatial resolution of ocean models more intrinsic variability is produced and, similarly, by analyzing the ratio of the externally forced

50 over the internally generated variability (Tang et al. (2020)) in the South China Sea, the external forcing is dominant for large scales, while most of the variability is internally generated for small scales.

Our paper addresses the predictability of the first kind for the Mediterranean Sea, focusing on the internal variability, following the methodology of Penduff et al. (2018), Leroux et al. (2018), Tang et al. (2020) and Lin et al. (2022).

The Mediterranean Sea is a semi-enclosed basin with an average depth of 1500 m and it is connected to the Atlantic Ocean

55 through the Strait of Gibraltar and to the Marmara Sea through the Dardanelles. The external forcings are the wind stress, responsible for the permanent gyres of the basin (Pinardi et al. (2015)), and the heat and water fluxes that control the overturning circulation (Pinardi et al. (2019)). Furthermore, ocean circulation in the Mediterranean Sea is characterized by significant interactions between different scales (Robinson et al. (2001)) and mesoscale variability is intense, producing 50 - 60 % of ocean kinetic energy variability (Bonaduce et al. (2021)). Mesoscales, for example, are associated with instabilities of the main flow

and they have a role in water mass transport across the basin (Demirov and Pinardi (2007)) and deep water formation processes (Waldman et al. (2017)).

We use a well-calibrated version of the Mediterranean Sea general circulation model used for short-term forecasting and we produce an ensemble of simulations using the same atmospheric forcing but different realistic initial conditions. First, we characterize the 3-D spatial distribution and the seasonal characteristics of the internal ocean variability over the entire basin. Secondly, we quantify the relative importance of the internal variability with respect to the atmospherically forced response using the *noise-to-signal ratio*. In the current analysis, the *signal* is identified with the mean of the ensemble of simulations whereas the *noise* or internal variability is approximated by the standard deviation of the ensemble members with respect to the mean. The questions we want to answer are: how large is the internal variability and what is its structure in the Mediterranean basin? What is the ratio between noise and signal?

The rest of the manuscript is organized as follows. The experimental setup is described in Section 2, alongside with the explanation of the rationale for the simulations and the statistical methods used. In Section 3 we show the evaluation of the quality of the ensemble experiment and in Section 4 the internal variability's spatial distribution, seasonality and dependence on depth are shown. Lastly, in Section 5 the stochastic variability is compared to the atmospherically forced variability and their relative importance is assessed. Conclusions are summarized in the last section.

2   Model set up and simulations

The model used in this work is one of the operational versions of the forecasting system of the Mediterranean Sea (Clementi et al. (2019), Coppini et al. (2023)) consisting of a coupled general circulation-wave model (Fig. 1) without tidal components. For the present work the wave component was disregarded. The model horizontal grid resolution is 1/24°(ca. 4 km) and has 141 unevenly spaced z* levels. The model is forced by momentum, water and heat fluxes computed through bulk formulae using the 1/10°horizontal-resolution operational analysis and forecast fields from the European Centre for Medium-Range Weather Forecasts (ECMWF). For more details on the specific model implementation, refer to Coppini et al. (2023).

 Following the idea in Penduff et al. (2018) and in Tang et al. (2020), an ensemble of 20 simulations of the Mediterranean Sea is generated with the same atmospheric conditions, but with different start dates and consequently different run times. Each simulation is initialized three months after the previous analyses starting from January 2016 to October 2020. Thus, each year four initial conditions are used to force simulations up to December 2021, as explained in Fig. 2. The differences between the simulations are generated by the evolution of the internal variability or, in other words, each simulation after three months has departed from the analysis which is used to initialize the model. The initial condition of a simulation with a later start date does not coincide with the simulation output at the same time. It is clear that the further back is the start date of the simulation, the longer has passed from the last analysis and internal nonlinearities have started to deviate the solution from the analysis. The same results could be obtained by just adopting different computing platforms, as proved in Lin et al. (2023a), since what is needed is just small disturbances.

It is important to notice that each ensemble member is driven through bulk formulae by identical atmospheric forcing function
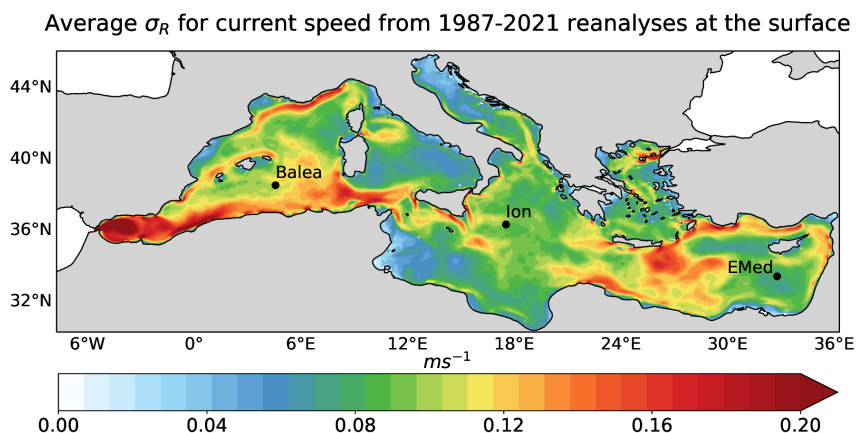
Figure 1. Average interannual spread σ_R in the Mediterranean Sea at the surface computed with the reanalyses from the period 1987 - 2021 (see Section 3). σ_R is computed as the spread of an ensemble composed of the current speed field of each year from 1987 to 2021. The dots indicate the locations that were chosen for the analysis: Balearic Islands (**Balea**), Ionian Sea (**Ion**) and Eastern Mediterranean Sea (**EMed**).

and atmospheric conditions, but variations in air-sea fluxes within the ensemble arise due to differences in oceanic variables (Bessières et al. (2017)). This configuration gives realistic results, but induces, for instance, an implicit relaxation of the SST

95 towards the same equivalent air temperature, thereby damping the SST spread (Barnier et al. (1995)).

The analysis is performed over the entire Mediterranean Sea at fixed depth levels (1 m, 20 m, 50 m, 100 m, 200 m, 500 m,
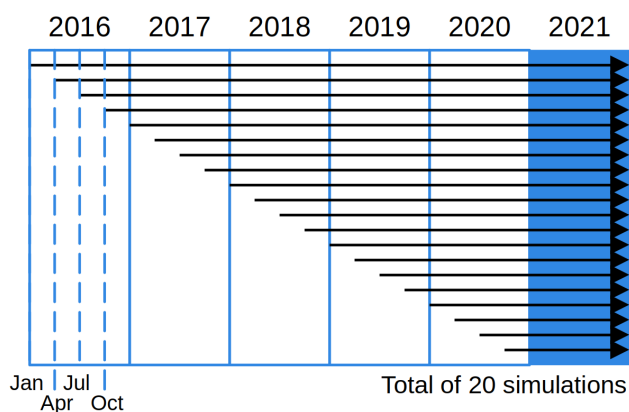
Figure 2. Scheme of the ensemble of 20 multi-year ocean simulations (black arrows). The blue box indicates the analyzed year.

1000 m) and at some locations, indicated by the dots in Fig. 1, that are chosen to characterize the entire basin from the Western to the Eastern side. Furthermore, starting from daily outputs, we focus on the seasonal timescale, in particular considering the four-month winter and summer seasons defined in Artegiani et al. (1997) for the Mediterranean region, i.e. January-April

100 (**JFMA**) and July–October (**JASO**), respectively.

2.1 Statistical methods

We employ basic ensemble statistics to measure the internal and forced variability of the ocean. The ensemble mean of the simulations is considered to represent the forced response of all members to the common forcing, hereafter indicated with the signal. Subtracting this quantity from each member we obtain the stochastic variations, uncorrelated between the members
105 (Penduff et al. (2018), Leroux et al. (2018)). Consequently, the internal ocean variability σ_I can be computed considering the discrepancy of each member from the ensemble average, i.e. the *ensemble standard deviation* or *ensemble spread* or *noise*, at each grid point (i, j):

$$\sigma_I(i,j,t) = \sqrt{\frac{1}{N-1} \sum_{n=1}^{N} [f_n(i,j,t) - f_{mean}(i,j,t)]^2} \tag{1}$$

where $N = 20$ is the ensemble size, f_n is the n-th member and f_{mean} is the ensemble mean. On the other hand, the atmospher-
110 ically forced variability σ_A, that is the variability shared by all simulations, is given by the evolution of the single-member means expressed by its temporal standard deviation:

$$\sigma_A(i,j;\tau) = \sqrt{\frac{1}{\tau-1} \sum_{t=1}^{\tau} [f_{mean}(i,j,t) - \bar{f}_{mean}(i,j)]^2} \tag{2}$$

where $\bar{f}_{mean}$ is the temporal average of the ensemble mean over the chosen period τ. In the present work, we use internal or intrinsic variability and ensemble spread interchangeably, the latter being the mathematical formulation of the former. To
115 compare (1) and (2), we consider the ratio, called *noise-to-signal ratio*, as the temporal average of the internal variability over the forced variability during the same period:

$$\frac{N}{S}(i,j;\tau) = \frac{\langle \sigma_I(i,j,t) \rangle_\tau}{\sigma_A(i,j;\tau)} \tag{3}$$

3 Variability: model output compared to reanalysis

To evaluate the quality of the model simulations, the ensemble members are compared to the reanalysis of the year 2021
120 (Escudier et al. (2021)) produced approximately with the same model but assimilating drifting profiles, satellite sea surface temperature, and altimetry.

For current velocities, we compared the internal variability found in the simulations and the standard deviation computed from the 2021 reanalysis, hereafter called σ_{2021}. We would like to verify that σ_I is not overestimated when compared to the natural variability represented by the standard deviation of the reanalysis. We found that the ensemble member internal variability is
125 generally smaller than both the interannual variability σ_R computed from the 1987 - 2021 reanalyses (Fig. 1) and the standard deviation σ_{2021} of the 2021 reanalysis (Fig. 3), with the only exception of the region around the Balearic Islands. We argue that the ensemble member's internal variability is comparable with the natural variability of the Mediterranean Sea at all depths and seasons.
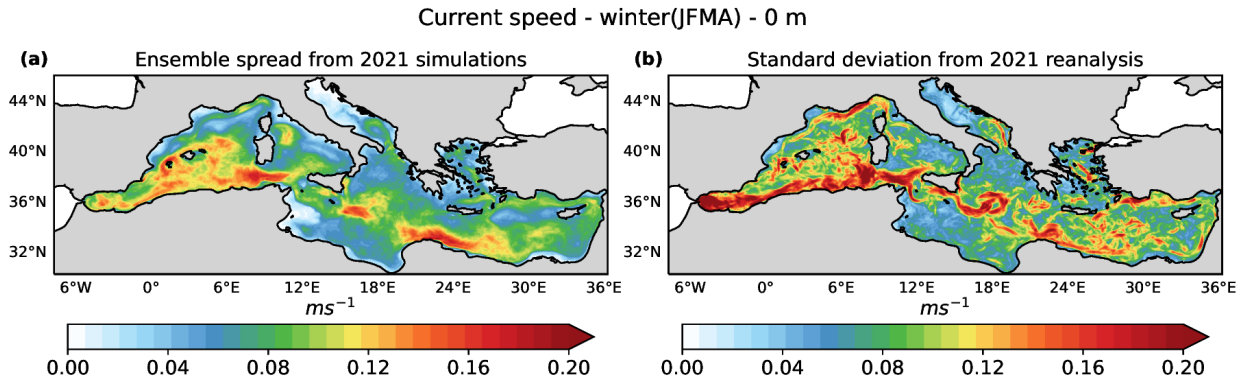
Figure 3. Comparison between the winter averaged ensemble spread σ_I with $N = 20$ **(a)** relative to current speed computed from the ensemble of simulations and the corresponding seasonal standard deviation σ_{2021} **(b)** obtained from the 2021 reanalysis.

Another evaluation of the ensemble spread is done by comparing it to the RMSE of the ensemble members with respect to the
130 2021 reanalysis r, as suggested in Fortin et al. (2014):

$$\sqrt{\overline{\sigma^2}} = \sqrt{\frac{N}{N+1}} RMSE \tag{4}$$

where $\sqrt{\overline{\sigma^2}} = \sqrt{\frac{1}{\tau} \sum_{t=1}^{\tau} var(t)}$ and $RMSE = \sqrt{\frac{1}{\tau} \sum_{t=1}^{\tau} (f_{mean}(t) - r(t))^2}$, with $\tau \to \infty$. It is important to note that both
Eq. 4 and 1 depend on the ensemble size N. Figure 4 (and Figure S1 in the Supplementary material) show the values of
the mean ensemble variance versus the RMSE for temperature and current speed, respectively, for each grid point averaged
135 over the entire year and at different depths. Points above the line described by Eq. 4 characterize an overdispersive ensemble,
whereas those below show an underdispersive ensemble. Overall, the present ensemble can be considered underdispersive. For
temperature, the ensemble variance and the uncertainty peak at roughly 30 m depth (Fig. 4), and in the case of current speed,
both the ensemble variance and the RMSE decrease with depth (Fig. S1).

Lastly, the ensemble spread and the noise-to-signal ratio were computed also for the year 2020 (see Fig. S12-S15 in Supple-
140 mentary material), but with only 16 simulations, resulting in the same findings as for 2021, proving that these are not peculiar
to the chosen year.

4   Characterization of internal variability

The ensemble spread for the current speed v and potential temperature T is shown in Fig. 5 at 30 m depth for both seasons (see
Fig. S4-S5 in Supplementary material for all depth levels). It is evident that internal variability for currents is high amplitude at
145 the surface and that in both seasons its spatial pattern is unchanged with depth while decreasing in intensity. In winter, the areas
with the highest intrinsic variability (0.12 - 0.15 ms^{-1}) are distributed along the southern parts of the basin while in summer,
an equally significant presence of internal variability is found in localized areas: in the Ionian Sea and in the westernmost part
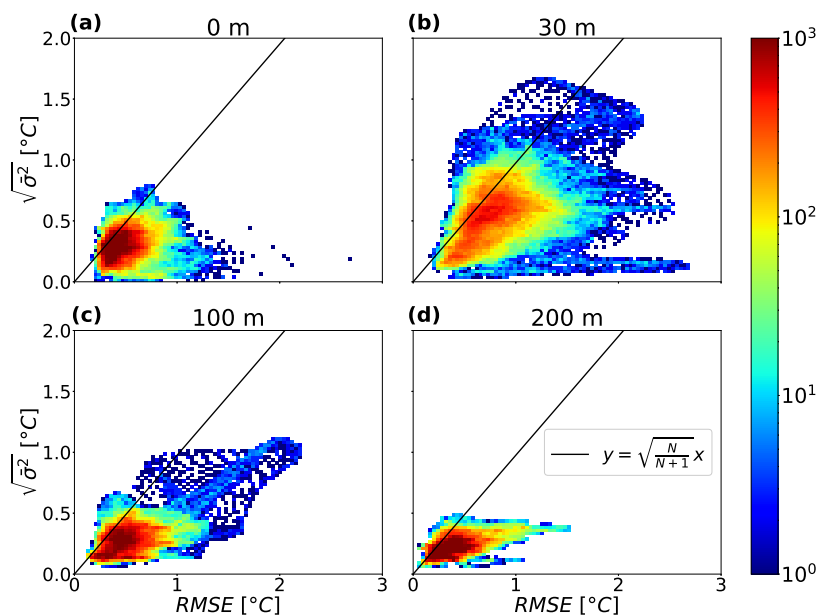
Figure 4. Ensemble dispersion relative to sea potential temperature: verification of Equation 4 averaged over the entire year 2021 for each grid point at the surface **(a)**, at 30 m **(b)**, at 100 m **(c)** and at 200 m **(d)**. The black line indicates the ideal relation expressed in Eq. 4.
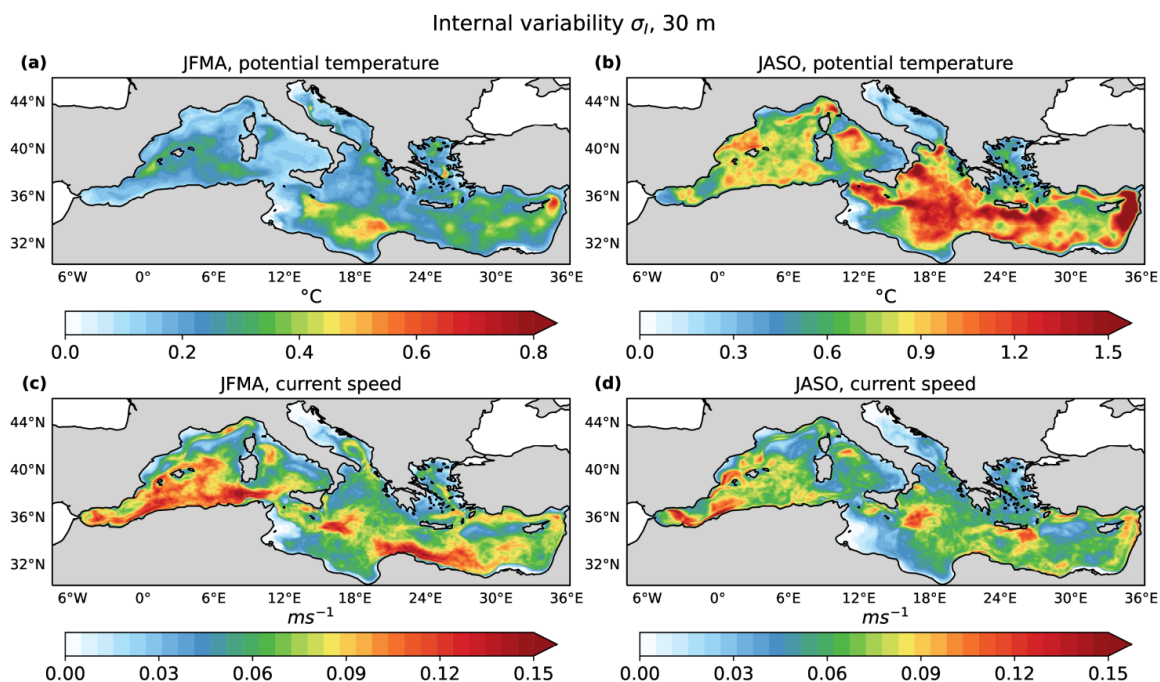
Figure 5. Seasonally averaged ensemble spread at 30 m depth for seawater potential temperature both in winter **(a)** and in summer **(b)**. Similarly for current speed in **(c)** and **(d)**.
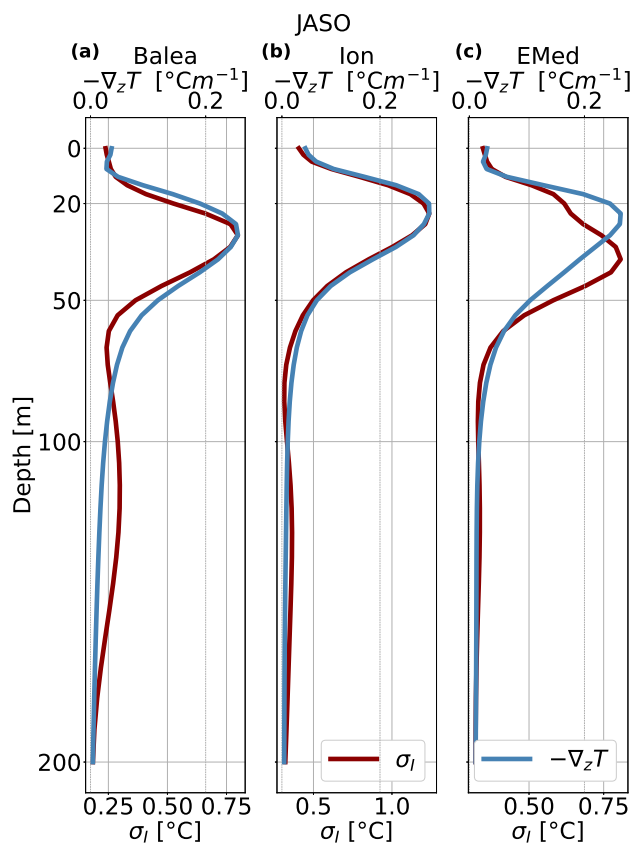
Figure 6. Seasonally averaged vertical profile of the ensemble spread σ_I (red) for potential temperature and of the vertical temperature gradient $-\nabla T_z$ (blue) in summer at **Balea (a)**, **Ion (b)** and **EMed (c)**.

of the basin. In both seasons, the Adriatic Sea and the Gulf of Gabes show the minimum values of the ensemble spread (less than 0.03 ms^{-1}).

150 For temperature, the ensemble spread exhibits a much more pronounced seasonality. In winter, the maximum values are of the order of 0.5 °C and are mainly located in the Eastern Mediterranean. Moreover, the spatial distribution of the spread remains practically constant along the water column up to the depth of 100 m. During summer the ensemble spread is largest at depths between 20 and 30 m (about 1.5 °C), which coincides with the upper seasonal thermocline center depth. The spread is again low in the Adriatic Sea and the Gulf of Gabes extended shelf areas. In fact, over shelf areas, the external forcing or signal exerts

155 a more significant influence with respect to deep ocean areas (Tang et al. (2020), Lin et al. (2022)). For depths greater than 100-200 m, the seasonal trend disappears for both current and temperature spread (see Fig. S6 in Supplementary Material).

 The vertical profile of the ensemble spread follows the vertical temperature gradient, as shown in Fig. 6. It peaks at the seasonal thermocline center depth, i.e. at the depth of the vertical temperature gradient maximum. In other words, the ensemble spread is greater where strong temperature gradients are present since small differences among the simulations are amplified by

160 the significant changes in the temperature field at these depths. However, the relation between ensemble spread and vertical temperature gradient varies depending on the location: in the Ionian Sea (Ion in Fig. 6) and in the Balearic Islands (Balea), the alignment between the two curves is notably robust. Conversely, in the Eastern Mediterranean (EMed), the peak of the temperature gradient occurs at approximately 20 m, whereas the maximum of σ_I is found at 40 m. We argue that the summer thermocline processes present large internal variability, therefore the thermocline depth tends to be different in each simulation.

5   Comparison between noise and signal

In order to quantify the relative importance of the internal variability with respect to the atmospherically forced response, the noise-to-signal ratio (Eq. 3) is computed. Figure 7 summarizes the basin-averaged vertical profile of *N/S* across the two seasons at the discrete depth levels defined in Section 2. The *N/S* for *T* is smaller than 1 up to 100 m (about 0.3 at the surface) and it increases with depth with greater values in winter in the surface layers and systematically larger values (approximately equal 170 to 6) in summer for the deeper part of the water column. On the other hand, the current speed's *N/S* is always greater than 1: it rises steadily in the first 50m, reaching a maximum at 200 m in summer and winter, and then slightly decreases with depth. Thus, even though σ_I has its maximum at some intermediate depth for *T* and it is maximum at the surface for *v*, the *N/S* is greater at depth due to the diminishing importance of the atmospheric forcing with increasing depth. Moreover, whereas for *v* the internal variability is always dominant, for *T* the atmospheric response has a dominant influence in the surface layers, 175 especially in winter.

As regards the spatial distribution of the noise-to-signal ratio, as expected the Adriatic Sea and the Gulf of Gabes are the regions with the smallest values of *N/S* for both *T* and *v*. For potential temperature (see Fig. 8) *N/S* in summer is less than 1 over the entire Mediterranean Sea at the surface, but it increases with depth, especially along the African coast in the Western Mediterranean and in the northern part of the Easter Mediterranean. In winter, instead, in the Ionian Sea, north of the Gulf 180 of Sidra, *N/S* is greater than unity and it tends to grow with depth mainly in this region and along the coast of Spain in the Western Mediterranean. Conversely, the model resolved mesoscale activity contributes to σ_I for *v* in vast open ocean areas of the basin. Figure 9, shows that *N/S* is higher than 1 in large open ocean areas offshore to vigorous northern and southern boundary currents (northern Liguro-Provencal current, the Algerian Current, The Asia Minore current, etc.). We argue that this internal variability is due to mesoscales. Some of the intense current regions, such as the Gibraltar inflow current and part of 185 the Liguro-Provencal current show a relevant contribution from external forcings, the Atlantic water inflow for the former and the wind stress curl for the latter, as documented by many authors (Herbaut et al. (1997), Molcard et al. (2002)). In the shallow areas of the Adriatic and Gulf of Gabes, where the external forcing is dominant, the mean flow probably fluctuates with the forcings and prevents the onset of instabilities and the production of internal variability.
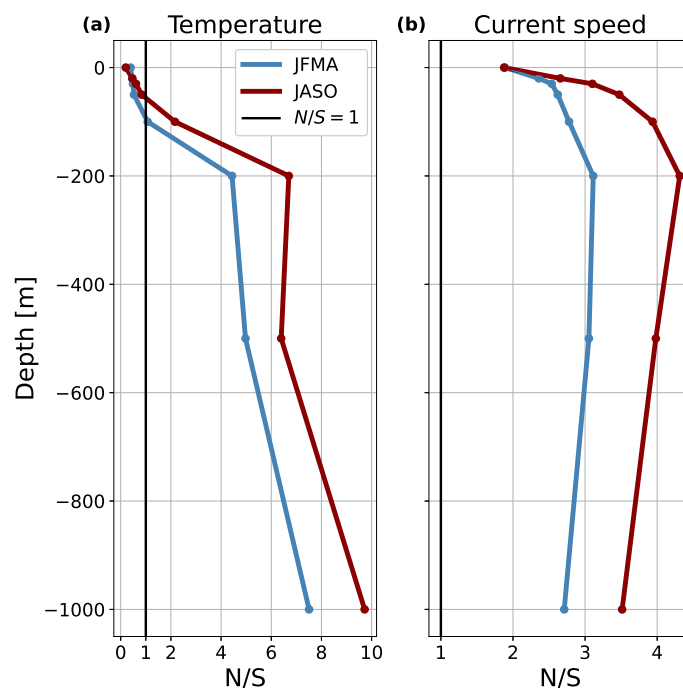
Figure 7. Vertical profile of the seasonally and spatially averaged noise-to-signal ratio for potential temperature **(a)** and current speed **(b)**. Red represents summer, whereas blue is winter and the black vertical lines correspond to $N/S = 1$.

6 Discussion and conclusions

190 In the present work, we used a simulation ensemble approach to study, for the first time in the Mediterranean Sea, the internal variability or noise versus the atmospherically forced signal. Producing an ensemble of 20 simulations of the Mediterranean Sea in 2021 with different start dates but forced by the same atmospheric conditions, we were able to characterize the internal ocean variability σ_I as opposed to the forced response of the ocean. Moreover, we used the noise-to-signal ratio *N/S* to measure the relative importance of the former compared to the latter. We characterized and quantified the internal variability

195 and *N/S* as regards their vertical profiles, seasonal cycle and spatial patterns for temperature and current speed. In general, the atmospherically forced response tends to decrease with depth and thrives instead in the extended shelf areas of the basin such as the Adriatic Sea and the Gulf of Gabes. Relative to temperature, the atmospheric forcing is dominant in the first 50 m of the water column in summer and in the first 100 m in winter. Furthermore, internal variability is dominant in most of the open ocean regions of the Mediterranean Sea, due to the intense mesoscale variability, offshore to intense northern and southern

200 mean current systems. To note is that some of the most intense currents have components that are externally forced, such as the Alboran current and segments of the Liguro-Provencal current system.

Lastly, the intrinsic variability shows a large seasonal cycle in temperature with a sharp maximum in summer at roughly 30 m depth and a much less pronounced one at about 100 m depth in winter. The vertical profile of the spread in summer is probably
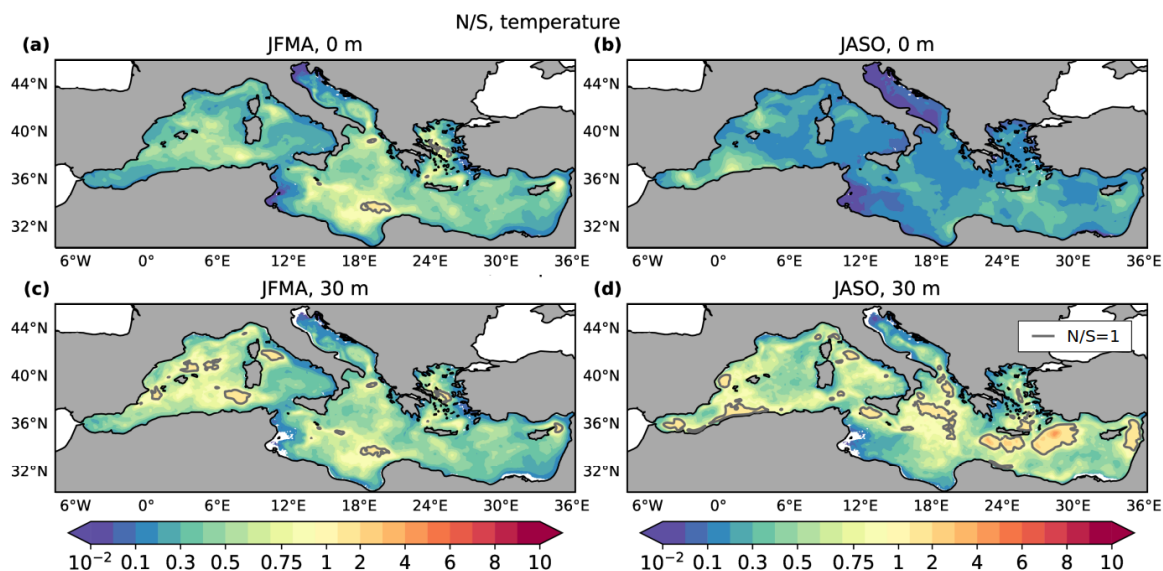
Figure 8. Seasonally averaged *N/S* for seawater potential temperature both in winter at the surface **(a)** and at 30 m depth **(c)**. Analogously for summer in **(b)** and **(d)**, respectively. The gray lines represent the isolines at *N/S* = 1.
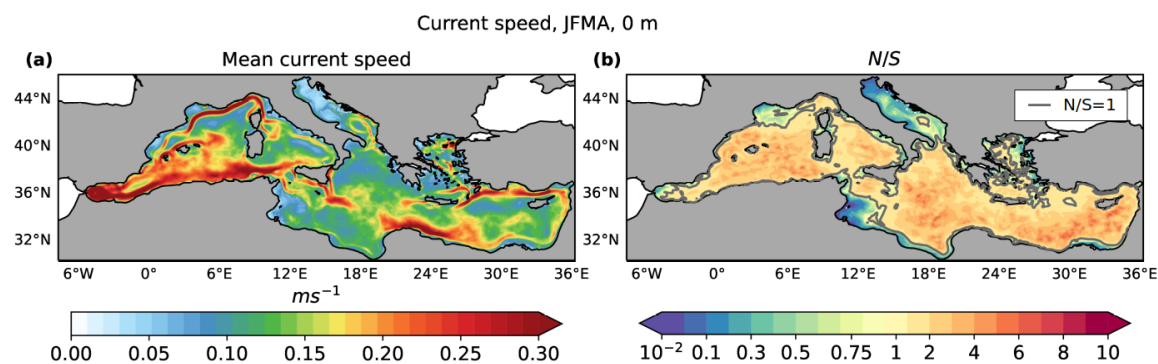
Figure 9. Seasonal average (winter, JFMA) at the surface of the ensemble mean **(a)** and of the *N/S* **(b)** for the speed of the current. The gray lines in the right plot represent the isolines at *N/S* = 1.

related to the large variability in the upper thermocline due to internal variability. Regarding current speed, the internal vari-
205 ability is dominant at all depths and largest at the surface.

The assessment of the internal oceanic variability is crucial for tackling the issue of estimating the ocean's intrinsic predictabil-
ity and comprehending the distinct roles of internal instabilities and external forcings in shaping ocean dynamics. Furthermore,
this research serves as an additional validation of the efficient yet straightforward nature of this ensemble statistics, derived
from the theory of stochastic climate models, whose aim is not to investigate specific hydrodynamic processes but to study the
210 system's properties and statistics (Lin et al. (2023b)). Moreover, the noise-to-signal ratio proves to be an effective diagnostic

indicator. Last but not least, the production of internal variability itself has been assessed, further proving the main idea behind stochastic climate models theory: in a dynamical system featuring the coexistence of diverse temporal scales and the possibility to distinguish between transient and mean components, variations can arise from their internal interactions without implying any external factor.

215   An extension of this analysis could involve the incorporation of tides into the general circulation model especially because tides have an important effect within the Gibraltar Strait (Gonzalez et al. (2021)), which could in turn result in differences in the generation and characterization of internal variability. For instance, the recent works by Lin et al. (Lin et al. (2022), Lin et al. (2024)) on the internal variability in the Bohai and Yellow Sea show that tidal forcing inhibits the generation of internal variability at large scales and that baroclinic instability might significantly drive the latter. Moreover, they suggest that the

220   memory of the system is a critical factor in the generation of internal variability at large scales: the spectrum of the intrinsic variability with tides is less *red* than the one without. Since in a first-order autoregressive process, as the mathematical formulation of stochastic climate models, the *redness* of the spectrum is a measure of the memory of the system, i.e. a measure of how long an anomaly will last once formed, this comparison shows that tides, and winter conditions, tends to decrease the system's memory, inhibiting anomalies to persist and upscale. The study of the importance of tides in the generation of internal

225   variability would be interesting to be redone in a deep basin such as the Mediterranean Sea.

Author contributions. All authors contributed to the design of this work. HvS, GL and NP formulated the initial problem idea, RB carried out all simulations and analyzed the output, and under the guidance of GL, RB developed the analysis tools. RAl authors contributed to the interpretation of the results

Competing interests. None

230   *Acknowledgements.* RB thanks GL, NP, and HvS for their guidance and mentorship throughout this work. Support for NP and GL work came from the H2020 EueoSea Project. The research presented in this paper was carried out on the supercomputer facilities of CMCC in Lecce (IT).

References

Adani, M., Dobricic, S., and Pinardi, N.: Quality assessment of a 1985–2007 Mediterranean Sea reanalysis, Journal of Atmospheric and Oceanic Technology, 28, 569–589, 2011.

Arbic, B. K., Müller, M., Richman, J. G., Shriver, J. F., Morten, A. J., Scott, R. B., Sérazin, G., and Penduff, T.: Geostrophic turbulence in the frequency–wavenumber domain: Eddy-driven low-frequency variability, Journal of Physical Oceanography, 44, 2050–2069, 2014.

Artegiani, A., Paschini, E., Russo, A., Bregant, D., Raicich, F., and Pinardi, N.: The Adriatic Sea general circulation. Part I: Air–sea interactions and water mass structure, Journal of physical oceanography, 27, 1492–1514, 1997.

Barnier, B., Siefridt, L., and Marchesiello, P.: Thermal forcing for a global ocean circulation model using a three-year climatology of ECMWF analyses, Journal of Marine Systems, 6, 363–380, 1995.

Bessières, L., Leroux, S., Brankart, J.-M., Molines, J.-M., Moine, M.-P., Bouttier, P.-A., Penduff, T., Terray, L., Barnier, B., and Sérazin, G.: Development of a probabilistic ocean modelling system based on NEMO 3.5: Application at eddying resolution, Geoscientific Model Development, 10, 1091–1106, 2017.

Bethoux, J., Gentili, B., Morin, P., Nicolas, E., Pierre, C., and Ruiz-Pino, D.: The Mediterranean Sea: a miniature ocean for climatic and environmental studies and a key for the climatic functioning of the North Atlantic, Progress in Oceanography, 44, 131–146, 1999.

Bonaduce, A., Cipollone, A., Johannessen, J. A., Staneva, J., Raj, R. P., and Aydogdu, A.: Ocean mesoscale variability: A case study on the Mediterranean Sea from a re-analysis perspective, Frontiers in Earth Science, 9, 724 879, 2021.

Büchmann, B. and Söderkvist, J.: Internal variability of a 3-D ocean model, Tellus A: Dynamic Meteorology and Oceanography, 68, 30 417, 2016.

Clementi, E., Pistoia, J., Escudier, R., Delrosso, D., Drudi, M., Grandi, A., Lecci, R., Cretí, S., Ciliberti, S., Coppini, G., et al.: Mediterranean Sea Analysis and Forecast (CMEMS MED-Currents, EAS5 system), 2019.

Coppini, G., Clementi, E., Cossarini, G., Salon, S., Korres, G., Ravdas, M., Lecci, R., Pistoia, J., Goglio, A. C., Drudi, M., et al.: The Mediterranean forecasting system. Part I: evolution and performance, EGUsphere, pp. 1–50, 2023.

Demirov, E. K. and Pinardi, N.: On the relationship between the water mass pathways and eddy variability in the Western Mediterranean Sea, Journal of Geophysical Research: Oceans, 112, 2007.

Escudier, R., Renault, L., Pascual, A., Brasseur, P., Chelton, D., and Beuvier, J.: Eddy properties in the Western Mediterranean Sea from satellite altimetry and a numerical simulation, Journal of Geophysical Research: Oceans, 121, 3990–4006, 2016.

Escudier, R., Clementi, E., Cipollone, A., Pistoia, J., Drudi, M., Grandi, A., Lyubartsev, V., Lecci, R., Aydogdu, A., Delrosso, D., et al.: A high resolution reanalysis for the Mediterranean Sea, Frontiers in Earth Science, 9, 702 285, 2021.

Fernández, V., Dietrich, D. E., Haney, R. L., and Tintoré, J.: Mesoscale, seasonal and interannual variability in the Mediterranean Sea using a numerical ocean model, Progress in Oceanography, 66, 321–340, 2005.

Ferrari, R. and Wunsch, C.: Ocean circulation kinetic energy: Reservoirs, sources, and sinks, Annual Review of Fluid Mechanics, 41, 253–282, 2009.

Fortin, V., Abaza, M., Anctil, F., and Turcotte, R.: Why should ensemble spread match the RMSE of the ensemble mean?, Journal of Hydrometeorology, 15, 1708–1713, 2014.

Gonzalez, N., Waldman, R., Sannino, G., Giordani, H., and Somot, S.: A new perspective on tidal mixing at the Strait of Gibraltar from a very high-resolution model of the Mediterranean Sea, in: EGU General Assembly Conference Abstracts, pp. EGU21–3971, 2021.

Harrison, D. and Robinson, A.: Energy analysis of open regions of turbulent flows—Mean eddy energetics of a numerical ocean circulation
270   experiment, Dynamics of Atmospheres and Oceans, 2, 185–211, 1978.

Harzallah, A., Alioua, M., and Li, L.: Mass exchange at the Strait of Gibraltar in response to tidal and lower frequency forcing as simulated
by a Mediterranean Sea model, Tellus A: Dynamic Meteorology and Oceanography, 66, 23 871, 2014.

Hasselmann, K.: Stochastic climate models part I. Theory, tellus, 28, 473–485, 1976.

Herbaut, C., Martel, F., and Crépon, M.: A sensitivity study of the general circulation of the Western Mediterranean Sea. Part II: the response
275   to atmospheric forcing, Journal of Physical Oceanography, 27, 2126–2145, 1997.

Hogan, E. and Sriver, R.: The effect of internal variability on ocean temperature adjustment in a low-resolution CESM initial condition
ensemble, Journal of Geophysical Research: Oceans, 124, 1063–1073, 2019.

Jochum, M. and Murtugudde, R.: Internal variability of the tropical Pacific Ocean, Geophysical research letters, 31, 2004.

Jochum, M. and Murtugudde, R.: Internal variability of Indian ocean SST, Journal of climate, 18, 3726–3738, 2005.

280   Le Traon, P. Y., Reppucci, A., Alvarez Fanjul, E., Aouf, L., Behrens, A., Belmonte, M., Bentamy, A., Bertino, L., Brando, V. E., Kreiner,
M. B., et al.: From observation to information and users: The Copernicus Marine Service perspective, Frontiers in Marine Science, 6, 234,
2019.

Leroux, S., Penduff, T., Bessières, L., Molines, J.-M., Brankart, J.-M., Sérazin, G., Barnier, B., and Terray, L.: Intrinsic and atmospherically
forced variability of the AMOC: Insights from a large-ensemble ocean hindcast, Journal of Climate, 31, 1183–1203, 2018.

285   Leroux, S., Brankart, J.-M., Albert, A., Brodeau, L., Molines, J.-M., Jamet, Q., Le Sommer, J., Penduff, T., and Brasseur, P.: Ensemble
quantification of short-term predictability of the ocean dynamics at kilometric-scale resolution: A Western Mediterranean test-case, Ocean
Science Discussions, 2022, 1–36, 2022.

Lin, L., von Storch, H., Guo, D., Tang, S., Zheng, P., and Chen, X.: The effect of tides on internal variability in the Bohai and Yellow Sea,
Dynamics of Atmospheres and Oceans, 98, 101 301, 2022.

290   Lin, L., von Storch, H., and Chen, X.: Seeding Noise in Ensembles of Marginal Sea Simulations—The Case of Bohai and Yellow Sea,
Advances in Computer and Communication, 4, 70–73, 2023a.

Lin, L., von Storch, H., and Chen, X.: The Stochastic Climate Model helps reveal the role of memory in internal variability in the Bohai and
Yellow Sea, Communications Earth & Environment, 4, 347, 2023b.

Lin, L., von Storch, H., Chen, X., Jiang, W., and Tang, S.: Link between the internal variability and the baroclinic instability in the Bohai and
295   Yellow Sea, Ocean Dynamics, 2024.

Lorenz, E.: Climatic predictability, GARP Publications series, pp. 132–136, 1975.

Lorenz, E. N.: Deterministic nonperiodic flow, Journal of atmospheric sciences, 20, 130–141, 1963.

McWilliams, J. C.: Modeling the oceanic general circulation, Annual Review of Fluid Mechanics, 28, 215–248, 1996.

Milliff, R. F., Bonazzi, A., Wikle, C. K., Pinardi, N., and Berliner, L. M.: Ocean ensemble forecasting. Part I: Ensemble Mediterranean winds
300   from a Bayesian hierarchical model, Quarterly Journal of the Royal Meteorological Society, 137, 858–878, 2011.

Molcard, A., Pinardi, N., Iskandarani, M., and Haidvogel, D.: Wind driven general circulation of the Mediterranean Sea simulated with a
Spectral Element Ocean Model, Dynamics of Atmospheres and Oceans, 35, 97–130, 2002.

Naranjo, C., Garcia-Lafuente, J., Sannino, G., and Sanchez-Garrido, J.: How much do tides affect the circulation of the Mediterranean Sea?
From local processes in the Strait of Gibraltar to basin-scale effects, Progress in Oceanography, 127, 108–116, 2014.

305   Penduff, T., Sérazin, G., Leroux, S., Close, S., Molines, J.-M., Barnier, B., Bessières, L., Terray, L., and Maze, G.: Chaotic variability of
ocean heat content: climate-relevant features and observational implications, Oceanography, 31, 63–71, 2018.

Pinardi, N. and Masetti, E.: Variability of the large scale general circulation of the Mediterranean Sea from observations and modelling: a review, Palaeogeography, Palaeoclimatology, Palaeoecology, 158, 153–173, 2000.

Pinardi, N., Bonazzi, A., Scoccimarro, E., Dobricic, S., Navarra, A., Ghiselli, A., and Veronesi, P.: Very large ensemble ocean forecasting experiment using the grid computing infrastructure, Bulletin of the American Meteorological Society, 89, 799–804, 2008.

Pinardi, N., Bonazzi, A., Dobricic, S., Milliff, R. F., Wikle, C. K., and Berliner, L. M.: Ocean ensemble forecasting. Part II: Mediterranean forecast system response, Quarterly Journal of the Royal Meteorological Society, 137, 879–893, 2011.

Pinardi, N., Zavatarelli, M., Adani, M., Coppini, G., Fratianni, C., Oddo, P., Simoncelli, S., Tonani, M., Lyubartsev, V., Dobricic, S., et al.: Mediterranean Sea large-scale low-frequency ocean variability and water mass formation rates from 1987 to 2007: A retrospective analysis, Progress in Oceanography, 132, 318–332, 2015.

Pinardi, N., Cessi, P., Borile, F., and Wolfe, C. L.: The Mediterranean sea overturning circulation, Journal of Physical Oceanography, 49, 1699–1721, 2019.

Pinardi, N., Estournel, C., Cessi, P., Escudier, R., and Lyubartsev, V.: Dense and deep water formation processes and Mediterranean overturning circulation, in: Oceanography of the Mediterranean Sea, pp. 209–261, Elsevier, 2023.

Pistoia, J., Pinardi, N., Oddo, P., Collins, M., Korres, G., and Drillet, Y.: Development of super-ensemble techniques for ocean analyses: the Mediterranean Sea case, Natural Hazards and Earth System Sciences, 16, 1807–1819, 2016.

Robinson, A. R., Leslie, W. G., Theocharis, A., and Lascaratos, A.: Mediterranean sea circulation, Ocean currents, 1, 2001.

Sannino, G., Carillo, A., Pisacane, G., and Naranjo, C.: On the relevance of tidal forcing in modelling the Mediterranean thermohaline circulation, Progress in Oceanography, 134, 304–329, 2015.

Sérazin, G., Penduff, T., Grégorio, S., Barnier, B., Molines, J.-M., and Terray, L.: Intrinsic variability of sea level from global ocean simulations: Spatiotemporal scales, Journal of Climate, 28, 4279–4292, 2015.

Simoncelli, S., F. C. P. N. G. A. D. M. O. P. . D. S.: Mediterranean Sea Physical Reanalysis (CMEMS MED-Physics) (Version 1) [Data set], Copernicus Monitoring Environment Marine Service (CMEMS), 2014.

Soldatenko, S. and Yusupov, R.: Predictability in Deterministic Dynamical Systems with Application to Weather Forecasting and Climate Modelling, in: Dynamical Systems-Analytical and Computational Techniques, p. 101, IntechOpen, 2017.

Su, F., Fan, R., Yan, F., Meadows, M., Lyne, V., Hu, P., Song, X., Zhang, T., Liu, Z., Zhou, C., et al.: Widespread global disparities between modelled and observed mid-depth ocean currents, Nature Communications, 14, 2089, 2023.

Tang, S., von Storch, H., Chen, X., and Zhang, M.: "Noise" in climatologically driven ocean models with different grid resolution, Oceanologia, 61, 300–307, 2019.

Tang, S., von Storch, H., and Chen, X.: Atmospherically forced regional ocean simulations of the South China Sea: scale dependency of the signal-to-noise ratio, Journal of Physical Oceanography, 50, 133–144, 2020.

von Storch, H., von Storch, J.-S., and Müller, P.: Noise in the climate system—ubiquitous, constitutive and concealing, Mathematics Unlimited—2001 and Beyond, pp. 1179–1194, 2001.

Waldman, R., Somot, S., Herrmann, M., Bosse, A., Caniaux, G., Estournel, C., Houpert, L., Prieur, L., Sevault, F., and Testor, P.: Modeling the intense 2012–2013 dense water formation event in the northwestern Mediterranean Sea: Evaluation with an ensemble simulation approach, Journal of Geophysical Research: Oceans, 122, 1297–1324, 2017.